



HAL
open science

N-centered, yet stable: an electronic structure investigation of FLP-type stabilized N₂O-based radicals

Andrea Orellana Ben Amor, Laure Vendier, Vincent César, Vincent Maurel, Julien Panetier, Nicolas Queyriaux

► To cite this version:

Andrea Orellana Ben Amor, Laure Vendier, Vincent César, Vincent Maurel, Julien Panetier, et al.. N-centered, yet stable: an electronic structure investigation of FLP-type stabilized N₂O-based radicals. 2025. ⟨hal-05536723⟩

HAL Id: hal-05536723

<https://hal.science/hal-05536723v1>

Preprint submitted on 4 Mar 2026

HAL is a multi-disciplinary open access archive for the deposit and dissemination of scientific research documents, whether they are published or not. The documents may come from teaching and research institutions in France or abroad, or from public or private research centers.

L'archive ouverte pluridisciplinaire HAL, est destinée au dépôt et à la diffusion de documents scientifiques de niveau recherche, publiés ou non, émanant des établissements d'enseignement et de recherche français ou étrangers, des laboratoires publics ou privés.



Distributed under a Creative Commons CC BY-NC-ND 4.0 - Attribution - Non-commercial use - No Derivative Works - International License

18 September 2025

N-centered, yet Stable: an Electronic Structure Investigation of FLP-type Stabilized N#O-Based Radicals

Andrea Orellana Ben Amor¹, Laure Vendier¹, Vincent César¹, Vincent Maurel³, Julien Panetier², Nicolas Queyriaux¹

1. Univ. Toulouse, CNRS, Laboratoire de Chimie de Coordination, Toulouse

2. Department of Chemistry, State University of New York at Binghamton, Binghamton, New York 13902, United States

3. IRIG, SyMMES, Univ. Grenoble Alpes, CEA, CNRS F-38000 Grenoble, France

Abstract

The electrochemical one-electron reduction of IDipp-N#O (IDipp = 1,3-bis(2,6-diisopropylphenyl)imidazol-2-ylidene) is inherently irreversible, highlighting the short-lived nature of the corresponding radical anion. However, stabilization by Lewis acidic boranes enables electrochemically reversible behavior, unlocking access to stable radical species. These radicals are synthesized via chemical reduction and fully characterized, revealing a highly N-centered nature alongside remarkable persistence at room temperature under an inert atmosphere. A comprehensive investigation of their electronic structure is presented, integrating electron paramagnetic resonance techniques (both continuous-wave and pulsed) with theoretical analysis to provide deeper insight into their properties.

Keywords

Radicals, N-Heterocyclic Carbenes (NHCs), Electron Paramagnetic Resonance (EPR), Nitrous Oxide Activation, DFT

N-centered, yet Stable: an Electronic Structure Investigation of FLP-type Stabilized N₂O-Based Radicals

Andrea Orellana Ben Amor,^[a] Laure Vendier,^[a] Vincent César,^[a] Vincent Maurel,^{*[b]} Julien Panetier^{*[c]} and Nicolas Queyriaux^{*[a]}

[a] A. Orellana Ben Amor, L. Vendier, V. César, N. Queyriaux
Univ. Toulouse, CNRS, LCC, Toulouse, France
nicolas.queyriaux@lcc-toulouse.fr

[b] V. Maurel
IRIG, SyMMES
Univ. Grenoble Alpes, CEA, CNRS
F-38000 Grenoble, France
vincent.maurel@cea.fr

[c] J. Panetier
Department of Chemistry
State University of New York at Binghamton
Binghamton, NY 13902 United States
panetier@binghamton.edu

Supporting information for this article is given via a link at the end of the document.

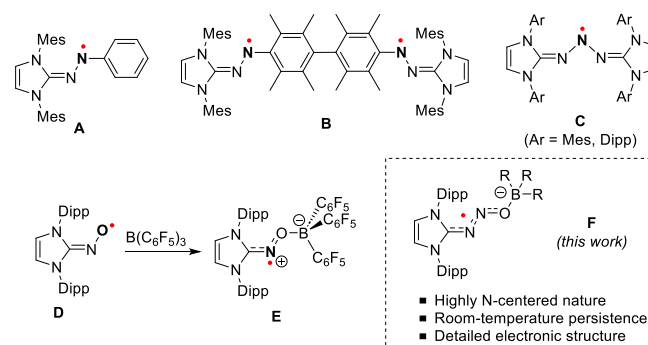
Abstract: The electrochemical one-electron reduction of IDipp-N₂O (IDipp = 1,3-bis(2,6-diisopropylphenyl)imidazol-2-ylidene) is inherently irreversible, highlighting the short-lived nature of the corresponding radical anion. However, stabilization by Lewis acidic boranes enables electrochemically reversible behavior, unlocking access to stable radical species. These radicals are synthesized *via* chemical reduction and fully characterized, revealing a highly N-centered nature alongside remarkable persistence at room temperature under an inert atmosphere. A comprehensive investigation of their electronic structure is presented, integrating electron paramagnetic resonance techniques (both continuous-wave and pulsed) with theoretical analysis to provide deeper insight into their properties.

Introduction

N-heterocyclic carbenes (NHCs) have recently emerged as powerful molecular tools capable of stabilizing N-centered radicals.^[1–3] Through a combination of both steric protection and π -accepting properties, NHCs greatly limit the reactivity of the radicals, typically resulting in persistent derivatives. In this context, a series of NHC-stabilized aminyl radicals has been isolated by the Severin group (Scheme 1, A).^[4] Those radicals – stable under an inert atmosphere – are characterized by a significant localization of the spin density of the unpaired electron (ca. 41%) on one of the nitrogen atoms of the diazenyl group. Open-shell diradicals, bridged by a permethylated biphenyl unit, were similarly isolated (Scheme 1, B). When exposed to air, these diradicaloid derivatives were found to be significantly less stable than their monoradical analogues. This was attributed to increased steric congestion, which limits the coplanarity of the diazenyl units with the adjacent arene ring, thereby accounting for low electron delocalization. Related triazenyl radicals were also synthesized by the Lee group (Scheme 1, C).^[5] Although

displaying a greater N-centered character (ca. 55%), the spin density of the radical is, again, computed to be significantly delocalized throughout the molecule.

Further stabilization of a radical species may also be achieved through the combined use of NHCs and Lewis acid partners, employing a Frustrated Lewis Pair (FLP) approach, which provides increased steric protection and electronic delocalization. Hence, Lee and co-workers demonstrated that the stabilization of an iminoxyl radical induced by a NHC alone was insufficient, resulting in progressive decomposition in solution.^[6] A dramatic increase in stability was achieved upon reaction with tris(pentafluorophenyl)borane (**1^a**), with the resulting zwitterionic radical displaying remarkable stability towards both air and moisture (Scheme 1, D→E).^[7]



Scheme 1. Molecular structures of NHC-stabilized N-centered radicals.

In γ -radiolysis, nitrous oxide (N₂O) has been used for a long time as a chain transfer agent, facilitating the increased generation of hydroxyl radicals in water.^[8,9] While undoubtedly involved in the process, the N₂O⁻ radical anion has never been experimentally evidenced. A notable result in this context was the *in situ* EPR characterization of a silyl-stabilized N₂O radical – embedded on a SiO₂ surface – by the group of Radtsig.^[10] From this perspective, it is therefore appealing to deploy NHC-based strategies that have

proven successful in stabilizing related aminyl and iminoxyl radicals to the N₂O motif. Interestingly, the group of Severin reported the preparation of NHC·N₂O adducts that may serve as convenient entry points in such an approach.^[11–13] Although they display a rich and diverse chemistry,^[14–19] their redox behavior remains virtually unexplored to date.

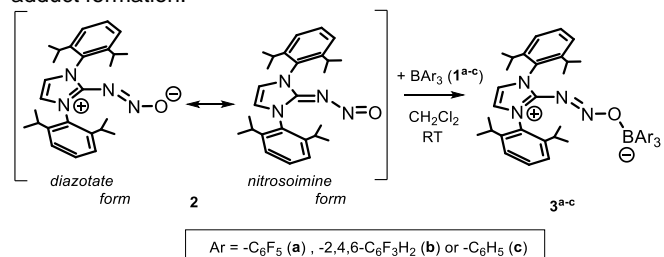
Here, we report the preparation of new FLP-type adducts of N₂O varying in the nature of their Lewis acid partners. Examination of their redox behavior specifically highlights the remarkable stability of the corresponding radical anions. Accordingly, such radicals were isolated and fully characterized. A specific focus has been dedicated to elucidating the electronic structures of these species through the use of electron paramagnetic resonance techniques and theoretical investigations. The aminyl nature of the N₂O-based radical is evidenced, with a high degree of N-centered character.

Results and Discussion

Adducts **3^{a-c}** were synthesized through a two-step synthetic route. 1,3-bis(2,6-diisopropylphenyl)-2*H*-imidazol-2-ylidene (IDipp) was initially exposed to N₂O following a reported procedure to produce the stable IDipp·N₂O adduct **2** (Scheme 2).^[11,12] Subsequent reactions with selected boranes (**1^{a-c}**) were carried out in dichloromethane at room temperature, resulting in the formation of adducts **3^{a-c}** in yields exceeding 80%. The relative Lewis acid strengths of these boranes were assessed using the Gutmann–Beckett method, employing triethylphosphine oxide (Et₃PO) as the Lewis base probe (refer to the Supporting Information for more details).^[20] When normalized to tris(pentafluorophenyl)borane (B(C₆F₅)₃, **1^a**: 100%), the values obtained for **1^{b-c}** reveal the selected boranes to cover a significant range of Lewis acidity (**1^b**: 85%, **1^c**: 57%).

Compounds **3^{a-c}** display spectroscopic signatures similar to related species.^[18,19] More specifically, the formation of adducts diagnostically influences chemical shifts of the imidazolium

backbone protons. In the ¹H NMR spectra, the corresponding singlet indeed experiences strong deshielding in comparison to the parent IDipp·N₂O compound (**2**: 7.25 ppm, **3^a**: 7.99 ppm, **3^b**: 7.78 ppm, **3^c**: 7.70 ppm). As the Lewis acid becomes stronger, an enhanced weight of the diazotate mesomeric form is expected in the hybrid structure of the corresponding adducts (Scheme 2). As a result, the resonance of the backbone protons is progressively shifted downfield, in line with an increased aromatic character. For comparison purposes, the 2-phenyl imidazolium analogue, **4·BF₄** (1,3-bis(2,6-diisopropylphenyl)-2-phenylimidazolium tetrafluoroborate), whose aromaticity is unambiguous, exhibits signals for these same protons at a value of 8.52 ppm. In the ¹³C{¹H} NMR spectra, the resonances for the carbene carbon atom of **3^{a-c}** are in the region of δ = 144 – 148 ppm, in good agreement with previous findings.^[18,19] ¹¹B{¹H} NMR spectra display sharp resonances at close-to-zero δ_B values, confirming the expected tetrahedral geometry around the boron atom. When present, signals of the fluorine atoms lying on the phenyl groups of the boranes are observed at chemical shifts consistent with adduct formation.



Scheme 2. Synthesis of the IDipp·N₂O·BAR₃ compounds **3^{a-c}**.

X-ray quality crystals were grown from THF/pentane solutions, allowing for X-ray diffraction analysis of all three compounds **3^{a-c}**. In all cases, the resulting structures confirm the coordination of the borane moiety to the IDipp·N₂O adduct **2** (Figure 1). The relevant bond lengths and angles for compounds **3^{a-c}** are summarized in Table 1, together with a comparison with the parent compound **2**.^[11]

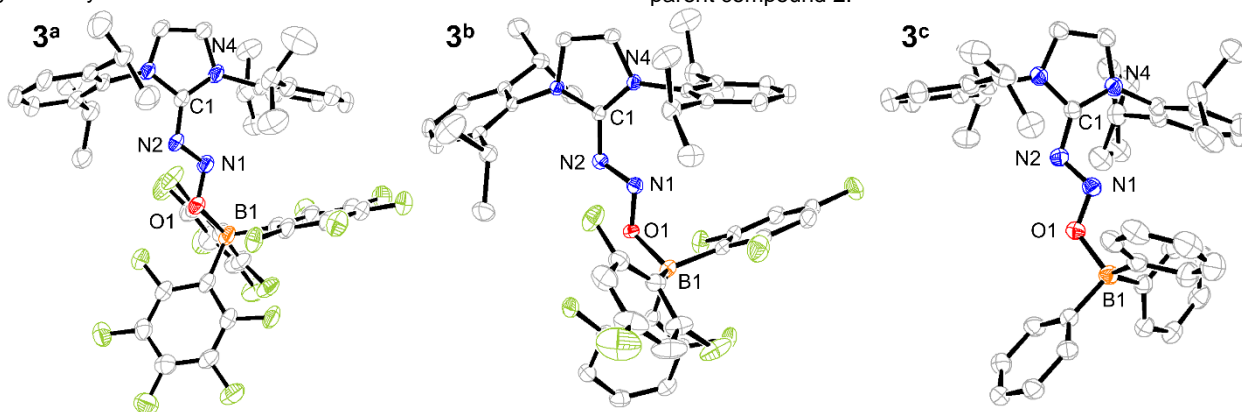


Figure 1. Molecular structures of **3^a** (left), **3^b** (centre) and **3^c** (right), as determined by X-ray diffraction. Thermal ellipsoids shown at the 50% probability level. Hydrogen atoms and solvent molecules were omitted for sake of clarity.

In detail, the N₂O motif adopts a bent geometry with its proximal nitrogen atom connected to the NHC carbon atom and its oxygen atom linked to the borane group. The N–N–O angles are in the range of 108–109°, thus showing increased bending compared to **2** (112.9°). Interestingly, the nature of the borane slightly – but

coherently – influences the N–N–O angle: the stronger the Lewis acid is, the more bent the motifs are. As a general trend, the N=N bonds tend to contract in **3^{a-c}** (1.27–1.28 Å) compared to **2** (1.35 Å), while the N–O bonds are elongated (1.30–1.32 Å in **3^{a-c}** vs 1.25 Å in **1**). Such a bond length inversion aligns well with the

results obtained other FLP-type adducts of N₂O.^[18,19,21,22] Upon increased acidity of the borane partner, enhanced coplanarity of the N₂O motif and the heterocycle is accessed: the solid angle formed by the mean planes associated with these two motifs is indeed shifting from 39.08° in **2** to 19.80, 23.55 and 35.35° for **3^{a-c}**, respectively.

Table 1. Selected bond lengths and angles for compounds **2** and **3^{a-c}**.

	2 ^[11]	3^a	3^b	3^c
N1–N2 (Å)	1.352(4)	1.283(2)	1.284(2)	1.277(2)
N1–O1 (Å)	1.250(4)	1.317(2)	1.313(2)	1.310(1)
B1–O1 (Å)	/	1.537(3)	1.551(2)	1.593(2)
C1–N2 (Å)	1.358(4)	1.374(3)	1.374(2)	1.376(2)
N2–N1–O1 (°)	112.9(3)	108.0(2)	108.4(1)	109.1(1)

To gain further insight into the electronic structures of compounds **3^{a-c}**, we conducted DFT calculations. Initial geometry optimizations were performed using the ωB97X-D^[23] functional in solution (tetrahydrofuran, ε = 7.4257) with the SMD approach (see the Supporting Information for more details).^[24] A good agreement was typically found between the X-ray and DFT geometries, with the most significant error being an underestimation of the N1–O1 bond distances by an average of 2.8% (Table S2). We note that, as observed experimentally, the computed N–N–O bond angle increases across the series in going from **3^a** (110.7°) to **3^c** (111.0°), consistent with **3^a** featuring the strongest Lewis acid borane moieties. Inspection of the frontier molecular orbitals in this series of compounds reveals that the lowest unoccupied molecular orbitals are primarily localized on the N₂O motif (see Supporting Information), suggesting that the one-electron reduced species will yield a N₂O radical.

We then investigated the electrochemical behavior of compounds **3^{a-c}**, along with the parent compound **2**, using cyclic voltammetry (CV). In dry THF (containing 0.1 M *n*Bu₄PF₆ as the supporting electrolyte), **2** exhibits two irreversible one-electron processes at E_{p,c} = -2.86 V vs Fc⁺/Fc and E_{p,a} = +0.68 V vs Fc⁺/Fc (Figure 2, green trace). Despite attempts to increase the scan rate (up to 1000 mV.s⁻¹) or decrease the temperature (down to 5°C), redox reversibility could not be achieved, even to a limited extent. Such a result suggests that the *in situ* electrogenerated radicals are highly unstable and further evolve in solution. Interestingly, dramatic differences were observed when recording the CVs of compounds **3^a** and **3^b** (Figure 2, blue and red traces, respectively). In both cases, a single quasi-reversible process was observed to occur at strongly anodically-shifted potentials of -1.70 and -1.93 V vs Fc⁺/Fc, for **3^a** and **3^b**, respectively. The borane moiety thus appears to have a dual effect: (i) by providing an increased steric hindrance and a partial electronic density delocalization, it firstly results in increased *kinetic stability* of the radical, ultimately leading to full reversibility recovery, and (ii), the decreased electronic density of the NHC–N₂O moiety simultaneously *lowers the energy required* to initiate electron transfer from the electrode, resulting in the observed anodic shift. As a result, the potential required can be tuned by the nature of the Lewis acid partner, as evidenced by the 230 mV gain in potential when switching from the partially fluorinated borane **1^b** to the perfluorinated one **1^a**.

Noteworthy, a similar beneficial effect of the addition of a Lewis-acidic borane was reported very recently in the one-electron reduction of NHC–CO₂ adducts.^[25] Linear trends were observed when plotting the variation of the anodic and cathodic peak currents (i_{p,a} and i_{p,c}) of the electrochemical process *versus* the square root of the scan rate (from 100 mV.s⁻¹ to 1000 mV.s⁻¹, see Supporting Information), confirming the compounds to freely diffuse in solution. Meanwhile, the CV of **3^c** suggests that the Lewis acidity of the borane **1^c** is insufficient to achieve efficient stabilization of the associated radical species. An irreversible process was indeed observed, similar to parent compound **2** (see Supporting Information). Interestingly, the 2-phenyl imidazolium **4⁺** displays a reversible one-electron process at a similar potential of -2.18 V vs Fc⁺/Fc (Figure 2, dark grey trace). As previously investigated by the Ghadwal group,^[26] the unpaired electron density of the resulting neutral radical was found to be partially located on the carbene carbon atom, with significant contributions from the carbon atoms of the aryl rings. This prior work thus questions the spin distribution in Lewis-acid stabilized radical anions [**3^{a-b}**]⁻, and more specifically, the extent of their delocalization.

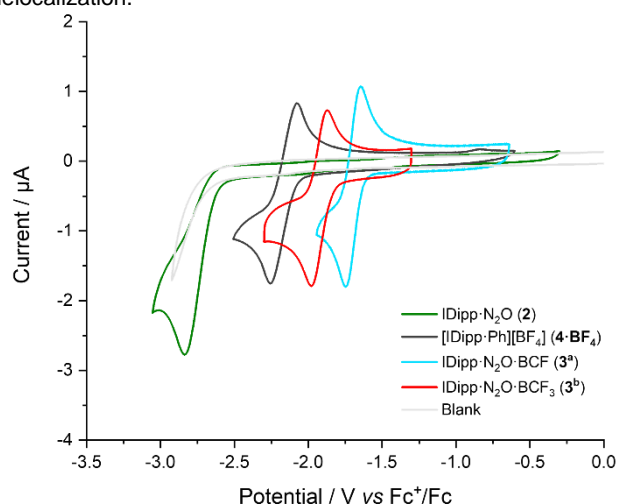


Figure 2. Cyclic voltammograms of compounds **2** (green trace), **3^a** (blue trace), **3^b** (red trace) and **4.BF₄** (dark grey trace), recorded in THF (0.1 M *n*Bu₄NPF₆) at a glassy carbon electrode (analyte concentration: 1 mM, scan rate: 100 mV s⁻¹).

To specifically address this point, we decided to synthesize the radical anions corresponding to the reduction of **3^a** and **3^b**. Encouraged by the reversible electrochemical behavior of those compounds on the CV timescale, we thus turned our attention to their preparative chemical reduction. Notably, one-electron reduction using potassium graphite (KC₈) in dry tetrahydrofuran enabled the isolation of the desired species in reasonable yields (>50%), as dark red solids. The structures of [**3^a**]⁻[K] and [**3^b**]⁻[K] were confirmed by single-crystal X-ray diffraction (Figure 3, together with relevant bond lengths and angles summarized in Table 2). Upon comparison with the parent neutral compounds, notable modifications are identified. Increased bending of the N–N–O angles is observed, with values as low as 103.2° in [**3^a**]⁻. To the best of our knowledge, it is one of the most acute angles reported for this structural motif so far, excluding cyclic derivatives.^[27–30] Meanwhile, the elongation of both the N–N and N–O bonds in the N₂O motif is observed. The N–N bonds are

observed in the range 1.34–1.35 Å in $[3^a]^-$ and $[3^b]^-$, which are typically halfway between single and double bonds and thus suggest an overall bond order of 1.5. As for the N–O bonds, they range from 1.40 to 1.41 Å, consistent with single bond character. Conversely, contraction of the B–O and $C_{\text{NHC}}\text{--N}$ bonds is observed, suggesting increased interactions within the FLP-type adducts that may account for the observed stability of the radicals. A

significant change in the structural features of these radicals lies in the increased coplanarity of the N_2O motif and the imidazolium ring: the dihedral angles associated with these two moieties shift from 19.80° and 23.55° in $3^{\text{a-b}}$ to 5.6° and 2.5° for $[3^{\text{a}}]^-$ and $[3^{\text{b}}]^-$, respectively. Similarly observed in radicals based on $\text{NHC}\text{--CO}_2\text{--borane}$ adducts,^[25] this overall flattening probably arises from increased conjugation within the radical.

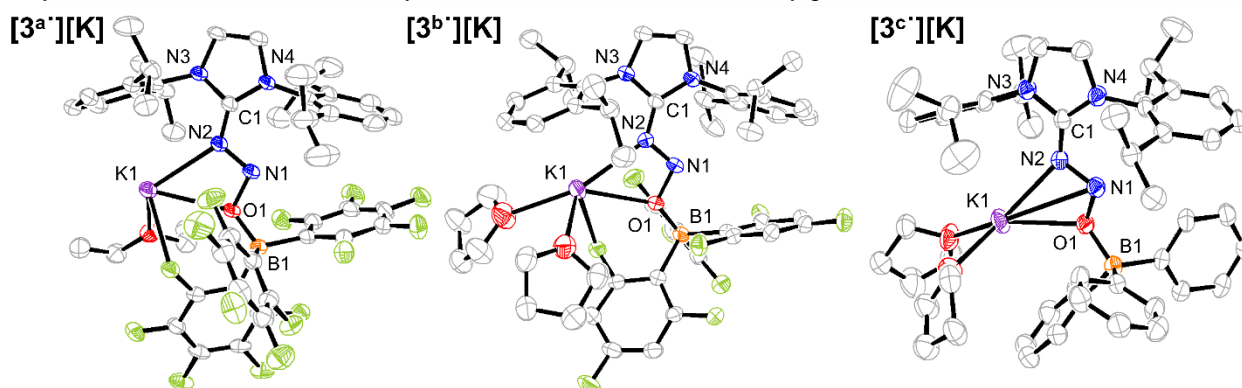


Figure 3. Molecular structures of $[3^{\text{a}}][\text{K}]$ (left), $[3^{\text{b}}][\text{K}]$ (centre) and $[3^{\text{c}}][\text{K}]$ (right), as determined by X-ray diffraction. Thermal ellipsoids shown at the 50 % probability level. Hydrogen atoms were omitted for sake of clarity.

Table 2. Selected bond lengths and angles for compounds $[3^{\text{a-c}}][\text{K}]$.

	$[3^{\text{a}}][\text{K}]$	$[3^{\text{b}}][\text{K}]$	$[3^{\text{c}}][\text{K}]$
N1–N2 (Å)	1.354(3)	1.340(4)	1.359(3)
N1–O1 (Å)	1.412(4)	1.400(3)	1.392(3)
B1–O1 (Å)	1.488(3)	1.493(4)	1.525(4)
C1–N2 (Å)	1.316(4)	1.312(4)	1.315(4)
N2–N1–O1 (°)	103.2	103.7	102.9

Interestingly, preparative one-electron reduction of 3^{c} under identical conditions allowed the isolation of a few dark red crystals. Suitable for X-ray diffraction, they allowed the characterization of the molecular structure of $[3^{\text{c}}][\text{K}]$ (Figure 3). No particular structural differences were noticed when compared with $[3^{\text{a}}][\text{K}]$ and $[3^{\text{b}}][\text{K}]$. At first glance, this result may seem somewhat puzzling, as it is inconsistent with the electrochemical data that support a low-stability radical. We suspect, however, that the potassium cation derived from the reduction using KC_8 plays a significant role in the stabilization of the radical. Mougel's group recently demonstrated that the presence of Lewis acidic alkali cations (K^+ , Rb^+ , Cs^+) is an effective strategy for stabilizing low-valent iron-sulfur cubanes.^[31] We believe that a similar scenario is at play here, with K^+ supplementing the low Lewis acidity of BPh_3 . Electron Paramagnetic Resonance (EPR) techniques were then used to gain further experimental insights into the electronic structure of the radicals $[3^{\text{a}}]^-$ and $[3^{\text{b}}]^-$ (Figure 4). The continuous wave (cw) EPR spectrum of $[3^{\text{b}}]^-$, recorded at room temperature, exhibits three main features separated by 37.1 MHz (1.32 mT), consistent with the strong isotropic hyperfine coupling computed by DFT ($A_{\text{iso,DFT}} = 29.1$ MHz) for the N1 nucleus. Each main feature of the cw-EPR exhibits 7 lines separated by 3–5 MHz and additional shoulders. To better identify such smaller couplings, the HYSCORE spectrum of $[3^{\text{b}}]^-$ was recorded at 70 K. In the left quadrant, two pairs of features are observed at $[+/-$

5.00; $-/+$ 8.71] and $[+/-$ 4.70; $-/+$ 2.45] MHz. Their position and shape correspond to those expected for the double quantum/double quantum and double quantum/single quantum transitions of a nitrogen nucleus having a mainly isotropic hyperfine interaction (weak values of T tensor components compared to A_{iso}). In this case, the hyperfine A_{iso} and quadrupolar K constants can be computed using the analysis developed by Dikanov and the relationship:^[32]

$$v_{\text{dq}\pm} = 2 [v_{\text{eff}\pm}^2 + K^2(3 + \eta^2)]^{1/2}$$

$$\text{with } v_{\text{eff}\pm} = \left| v_{14\text{N}} \pm \frac{a}{2} \right|$$

This analysis provides hyperfine coupling of $A_{\text{iso,exp}} = 5.9$ MHz and a quadrupolar interaction in the range $0.81 < K < 0.93$ (in MHz), in very good agreement with the values computed by DFT ($A_{\text{iso,DFT}} = -5.4$ MHz, $K_{\text{DFT}} = 0.87$ MHz) for N2 (Table 3). In the right quadrant two very intense features are observed at $[+/-$ 4.71; $-/+$ 2.44] MHz. They are typical of nitrogen nuclei with hyperfine coupling constants close to the so-called cancellation condition: $A/2 \sim \nu_{14\text{N}}$ (Nuclear Larmor frequency for ^{14}N , 1.07 MHz at 3460 G). These signals can be attributed to the N3 and N4 nuclei, as determined by DFT computations, since it is clear that, for some orientations of $[3^{\text{b}}]^-$ vs. magnetic field, the hyperfine couplings of these nuclei fulfill the cancellation condition. However, the pronounced anisotropic character of the hyperfine tensors of N3 and N4 predicted by DFT computations (see the higher values of T tensors for N3 and N4 compared with N2 in Table 2), does not allow the use of the same quantitative analysis as for the N2 nucleus. The last two features are observed centered on the diagonal at 1.6 MHz and 4.8 MHz, which can be attributed, respectively, to the ^{10}B and ^{11}B isotopes of the boron nucleus. The signal centered at 4.8 MHz extends over a range of ~3–4 MHz in the antidiagonal direction, in good agreement with the small and anisotropic hyperfine interaction computed by DFT for this ^{11}B nucleus (Table 3). Noteworthy, no signal was observed that could be attributed to ^1H or ^{19}F nuclei, except for a very weak signal

close to the diagonal at 14.7 MHz, corresponding to very small hyperfine couplings (< 2 MHz; see full scale spectrum in the Supplementary Information).

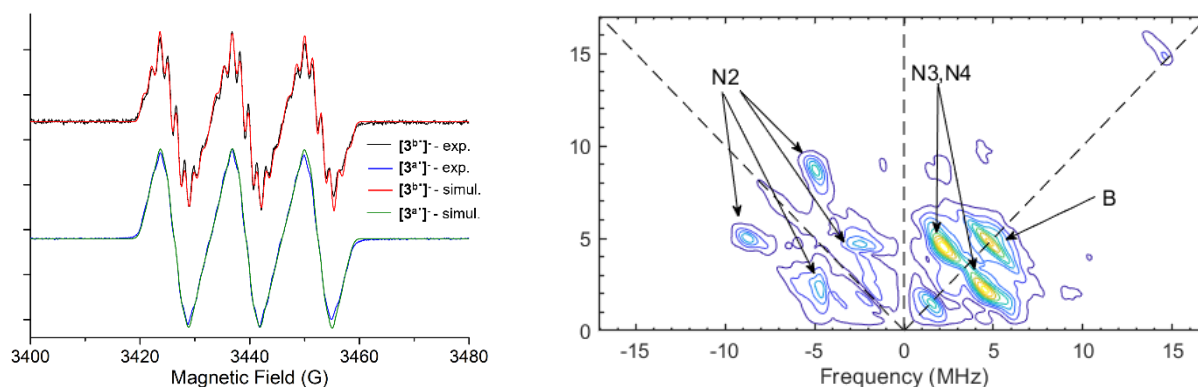


Figure 4. EPR spectra of $[3a]^{•-}$ and $[3b]^{•-}$, in solution at room temperature and the numerical simulation (left) and HYSCORE spectrum of $[3b]^{•-}$ recorded at $T=70K$ (right).

		N1	N2	N3	N4	B	linewidth
$[3a]^{•-}$	$A_{iso,exp} / A_{iso,DFT}$	36.8 / 28.7	EPR 4.3/-4.4 HYSCORE 5.9	3.6 / 4.0	4.1 / 4.3	1.4 / -3.7	4.7
	T_{DFT}	[-29.3 -30.5 59.8]	[2.8 -0.7 -2.1]	[-4.4 -4.6 9.0]	[-4.1 -3.8 7.9]	[2.7 -1.2 -1.5]	
	K_{exp} / K_{DFT}	n.m. / 1.13	0.81<K<0.93 / 0.86	n.m. / -1.13	n.m. / -1.14	n.m. / 0.04	
$[3b]^{•-}$	$A_{iso,exp} / A_{iso,DFT}$	37.1 / 28.7	EPR 4.6 / -5.3 HYSCORE 5.9	3.8 / 3.8	4.5 / 4.4	1.7 / -4.1	3.4
	T_{DFT}	[-29.3 -30.4 59.7]	[1.2 0.1 -1.3]	[-4.2 -4.4 8.6]	[-4.0 -3.6 7.6]	[2.8 -1.3 -1.5]	
	K_{exp} / K_{DFT}	n.m. / 1.11	0.81<K<0.93 / 0.86	n.m. / -1.15	n.m. / -1.15	n.m. / 0.06	

Table 3. EPR parameters (in MHz) of $[3a]^{•-}$ and $[3b]^{•-}$ obtained by numerical simulation of spectra shown in Figure 4 and comparison with DFT-computed ones

Moreover, the experimental room-temperature cw-EPR spectrum can be numerically simulated (Easyspin software package), considering only the isotropic hyperfine coupling of N1, N2, N3, N4 and B nuclei. The agreement between the numerically fitted and the experimental spectrum is excellent. The A_{iso} values extracted from this simulation match reasonably well those computed by DFT, which, in addition to the HYSCORE experiment, further validates experimentally the electronic structure of $[3b]^{•-}$ calculated by DFT.

EPR and HYSCORE investigations of the radical $[3a]^{•-}$ yielded very similar results. The HYSCORE spectrum is similar to that of $[3b]^{•-}$ (see Supporting Information). The EPR spectrum of $[3a]^{•-}$ recorded at room temperature is less resolved than the spectrum of $[3b]^{•-}$, but careful numerical simulation leads to very similar hyperfine coupling constants in good agreement with DFT computations. As expected, the plot of the Mulliken spin density for the one-electron reduced species indicates that most of the electron density is localized on the N_2O moiety (e.g., $\rho(N_2O) = 0.71$, Figure 5A), in agreement with the EPR properties. We also note that the frontier molecular orbitals for $[3a]^{•-}$ indicate that the highest occupied molecular orbital, which is located in the α -space, involves a π^* orbital on the N_2O moiety, consistent with the experimentally observed elongation of both the N-N and N-O bonds. Taken together, structural information, spectroscopic data, and DFT calculations all point towards the reduced species being best described as aminyl radicals (Figure 5B).

Interestingly, we found that the radical anion $[3b]^{•-}$ exhibits remarkable stability in solution at room temperature, persisting for weeks under an inert atmosphere (based on cw-EPR and UV-Vis spectroscopy measurements). In contrast, exposure to oxygen leads to immediate re-oxidation to the neutral adduct $[3b]$, likely *via* an outer-sphere electron transfer mechanism. While extended stability has been reported for structurally related radicals, it remains surprising in this case due to the strongly N-centered character of the radical, which is typically associated with short-lived, highly reactive species. These results, therefore, point to an important kinetic stabilization capable of balancing the thermodynamic drivers typically associated with strongly localized organic radicals.^[33] This stability is likely due to effective steric protection of the spin density within a highly congested molecular environment.

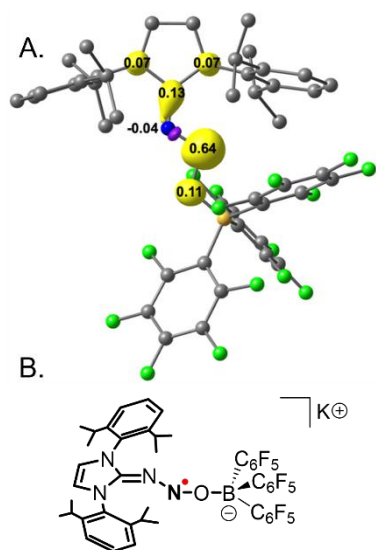


Figure 5. (A) Isosurface (0.007 au) plot of the Mulliken spin population of the one-electron reduced species $[3^{*\bullet-}]$. Hydrogen atoms have been omitted for clarity. (B) Corresponding Lewis representation of the aminyl radical $[3^{*\bullet-}]$.

Conclusion

In summary, we report the synthesis, isolation and full characterization of the first molecular examples of N_2O -based radical anions. Access to these species, best described as aminyl-type radicals, was enabled by a FLP-type strategy combining N-heterocyclic carbenes with boron-based Lewis acids. Electrochemical studies demonstrated that the nature and strength of the Lewis acid partner directly influence both the redox properties and the stability of the resulting radicals. A combination of CW-EPR spectroscopy, HYSCORE experiments, and DFT calculations, confirmed that the spin density is primarily localized on the central nitrogen atom, yielding a highly N-centered radical. Remarkably, despite this localization, the radicals display significant persistence in solution under inert atmosphere – a feature attributed to the substantial steric protection afforded by the surrounding molecular environment.

Supporting Information

General information, synthetic procedures, characterization data of all new compounds, computational details, EPR additional spectra, supplementary electrochemical measurements and detailed crystallographic data can be found in the Supporting Information. The authors have also cited additional references within the Supporting Information.^[11,12,23,24,34–55]

Acknowledgements

Dr. Baptiste Martin is acknowledged for preliminary EPR experiments. Dr. Alix Sournia-Saquet is gratefully acknowledged for granting access to the electrochemistry facility at LCC. Dr. Sébastien Bontemps is thanked for fruitful discussions. Dr. Dmitry Valyaev is kindly acknowledged for providing compound **4-BF₄**.

N.Q. would like to thank the CNRS and the ANR (grant ANR-24-CE07-5771-01) for financial support. A.O.B. acknowledges funding from the University of Toulouse for her PhD fellowship. Financial support from the IR INFRANALYTICS FR2054 for conducting the research is gratefully acknowledged. This material is also based upon work supported by the National Science Foundation under Grant No. CHE-2400072.

Keywords: radical • N-heterocyclic carbene • EPR spectroscopy • nitrous oxide activation • Frustrated Lewis Pairs (FLP) • DFT

- [1] Y. Kim, E. Lee, "Stable Organic Radicals Derived from N-Heterocyclic Carbenes" *Chemistry – A European Journal* **2018**, *24*, 19110–19121.
- [2] H. Song, E. Pietrasiak, E. Lee, "Persistent Radicals Derived from N-Heterocyclic Carbenes for Material Applications" *Acc. Chem. Res.* **2022**, *55*, 2213–2223.
- [3] S. Gao, F. Li, "Neutral Stable Nitrogen-Centered Radicals: Structure, Properties, and Recent Functional Application Progress" *Advanced Functional Materials* **2023**, *33*, 2304291.
- [4] L. Y. M. Eymann, A. G. Tskhovrebov, A. Sienkiewicz, J. L. Bila, I. Živković, H. M. Rønnow, M. D. Wodrich, L. Vannay, C. Corminboeuf, P. Pattison, E. Solari, R. Scopelliti, K. Severin, "Neutral Aminyl Radicals Derived from Azoimidazolium Dyes" *J. Am. Chem. Soc.* **2016**, *138*, 15126–15129.
- [5] J. Back, J. Park, Y. Kim, H. Kang, Y. Kim, M. J. Park, K. Kim, E. Lee, "Triazenyl Radicals Stabilized by N-Heterocyclic Carbenes" *J. Am. Chem. Soc.* **2017**, *139*, 15300–15303.
- [6] J. Park, H. Song, Y. Kim, B. Eun, Y. Kim, D. Y. Bae, S. Park, Y. M. Rhee, W. J. Kim, K. Kim, E. Lee, "N-Heterocyclic Carbene Nitric Oxide Radicals" *J. Am. Chem. Soc.* **2015**, *137*, 4642–4645.
- [7] Y. Kim, E. Lee, "An air-stable N-heterocyclic carbene iminoxyl borate radical zwitterion" *Chem. Commun.* **2018**, *54*, 6824–6827.
- [8] P. Popov, N. Getoff, J. Grodkowski, Z. Zimek, A. G. Chmielewski, "Steady-state radiolysis and product analysis of aqueous diphenyloxide in the presence of air and N_2O " *Radiation Physics and Chemistry* **2004**, *69*, 39–44.
- [9] M. I. Al-Sheikhly, H.-P. Schuchmann, C. von Sonntag, "γ-Radiolysis of N_2O -saturated Formate Solutions. A Chain Reaction." *International Journal of Radiation Biology and Related Studies in Physics, Chemistry and Medicine* **1985**, DOI 10.3109/rab.47.4.457.
- [10] V. A. Radtsig, "Free Radical Reactions of N_2O Molecules" *Kinetics and Catalysis* **2001**, *42*, 631–652.
- [11] A. G. Tskhovrebov, E. Solari, M. D. Wodrich, R. Scopelliti, K. Severin, "Covalent Capture of Nitrous Oxide by N-Heterocyclic Carbenes" *Angewandte Chemie International Edition* **2012**, *51*, 232–234.
- [12] A. G. Tskhovrebov, B. Vuichoud, E. Solari, R. Scopelliti, K. Severin, "Adducts of Nitrous Oxide and N-Heterocyclic Carbenes: Syntheses, Structures, and Reactivity" *J. Am. Chem. Soc.* **2013**, *135*, 9486–9492.
- [13] L. Y. M. Eymann, R. Scopelliti, F. T. Fadaei, G. Cecot, E. Solari, K. Severin, "Fixation of nitrous oxide by mesoionic and carbanionic N-heterocyclic carbenes" *Chem. Commun.* **2017**, *53*, 4331–4334.
- [14] L. Y. M. Eymann, R. Scopelliti, F. F. Tirani, K. Severin, "Synthesis of Azo Dyes from Mesoionic Carbenes and Nitrous Oxide" *Chemistry – A European Journal* **2018**, *24*, 7957–7963.
- [15] L. Y. M. Eymann, P. Varava, A. M. Shved, B. F. E. Curchod, Y. Liu, O. M. Planes, A. Sienkiewicz, R. Scopelliti, F. Fadaei Tirani, K. Severin, "Synthesis of Organic Super-Electron-Donors by Reaction of Nitrous Oxide with N-Heterocyclic Olefins" *J. Am. Chem. Soc.* **2019**, *141*, 17112–17116.
- [16] A. G. Tskhovrebov, L. C. E. Naested, E. Solari, R. Scopelliti, K. Severin, "Synthesis of Azoimidazolium Dyes with Nitrous Oxide" *Angewandte Chemie International Edition* **2015**, *54*, 1289–1292.
- [17] A. G. Tskhovrebov, E. Solari, M. D. Wodrich, R. Scopelliti, K. Severin, "Sequential N–O and N–N Bond Cleavage of N-Heterocyclic Carbene-Activated Nitrous Oxide with a Vanadium Complex" *J. Am. Chem. Soc.* **2012**, *134*, 1471–1473.
- [18] A. Thakur, P. K. Vardhanapu, G. Vijaykumar, P. Kumar Hota, S. K. Mandal, "Abnormal N-Heterocyclic-Carbene-Mediated Fixation of CO_2

- and N₂O, and the Activation of Tetrahydro-furan and Tetrahydrothiophene under Ambient Conditions" *European Journal of Inorganic Chemistry* **2016**, 2016, 913–920.
- [19] E. Theuergarten, T. Bannenberg, M. D. Walter, D. Holschumacher, M. Freytag, C. G. Daniliuc, P. G. Jones, M. Tamm, "Computational and experimental investigations of CO₂ and N₂O fixation by sterically demanding N-heterocyclic carbenes (NHC) and NHC/borane FLP systems" *Dalton Trans.* **2014**, 43, 1651–1662.
- [20] S. Keess, A. Simonneau, M. Oestreich, "Direct and Transfer Hydrosilylation Reactions Catalyzed by Fully or Partially Fluorinated Triarylboranes: A Systematic Study" *Organometallics* **2015**, 34, 790–799.
- [21] E. Otten, R. C. Neu, D. W. Stephan, "Complexation of Nitrous Oxide by Frustrated Lewis Pairs" *J. Am. Chem. Soc.* **2009**, 131, 9918–9919.
- [22] R. C. Neu, E. Otten, A. Lough, D. W. Stephan, "The synthesis and exchange chemistry of frustrated Lewis pair–nitrous oxide complexes" *Chem. Sci.* **2010**, 2, 170–176.
- [23] J.-D. Chai, M. Head-Gordon, "Long-range corrected hybrid density functionals with damped atom–atom dispersion corrections" *Phys. Chem. Chem. Phys.* **2008**, 10, 6615–6620.
- [24] A. V. Marenich, C. J. Cramer, D. G. Truhlar, "Universal Solvation Model Based on Solute Electron Density and on a Continuum Model of the Solvent Defined by the Bulk Dielectric Constant and Atomic Surface Tensions" *J. Phys. Chem. B* **2009**, 113, 6378–6396.
- [25] A. Morales, C. Gonçalves, A. Sournia-Saquet, L. Vendier, A. Lledós, O. Baslé, S. Bontemps, "Single electron reduction of NHC–CO₂–borane compounds" *Chem. Sci.* **2024**, 15, 3165–3173.
- [26] D. Rottschäfer, B. Neumann, H.-G. Stammler, M. van Gastel, D. M. Andrada, R. S. Ghadwal, "Crystalline Radicals Derived from Classical N-Heterocyclic Carbenes" *Angewandte Chemie International Edition* **2018**, 57, 4765–4768.
- [27] D. Grosse, L. Harrison, K. Turnbull, "3-{5-Bromo-2-[(tri-phenyl-phosphanyl-iden)amino]-phen-yl}-4,5-di-hydro-1,2,3-oxa-diazol-3-ylum-5-olate" *Acta Cryst E* **2013**, 69, o1196–o1196.
- [28] T. J. King, P. N. Preston, J. S. Suffolk, K. Turnbull, "Crystal and molecular structures of sydnones, 4,5-diphenylisodnydnone, and mesoionic tetrazoles" *J. Chem. Soc., Perkin Trans. 2* **1979**, 1751–1757.
- [29] D. Dumitrescu, S. Shova, C. Draghici, M. M. Popa, F. Dumitrascu, "Synthesis of 1-(2-Fluorophenyl)pyrazoles by 1,3-Dipolar Cycloaddition of the Corresponding Sydnones" *Molecules* **2021**, 26, 3693.
- [30] G. Fischer, D. Hunkler, H. Prinzbach, G. Rihs, H. Fritz, "The azoxy(azo)-chromophore as π₂-component in photo [2+2] cycloaddition reactions" *Tetrahedron Letters* **1984**, 25, 2459–2462.
- [31] L. Grunwald, M. Inoue, P. C. Carril, M. Wörle, V. Mougél, "Gated electron transfers at synthetic iron-sulfur cubanes" *Chem* **2023**, 0, DOI 10.1016/j.chempr.2023.09.023.
- [32] Q. Lam, C. Van Stappen, Y. Lu, S. A. Dikanov, "HYSCORE and QM/MM Studies of Second Sphere Variants of the Type 1 Copper Site in Azurin: Influence of Mutations on the Hyperfine Couplings of Remote Nitrogens" *J. Phys. Chem. B* **2024**, 128, 3350–3359.
- [33] S. S. S. V, P. C. S. John, R. S. Paton, "A quantitative metric for organic radical stability and persistence using thermodynamic and kinetic features" *Chem. Sci.* **2021**, 12, 13158–13166.
- [34] C. Wang, G. Erker, G. Kehr, K. Wedeking, R. Fröhlich, "Synthesis, Structural Features, and Formation of Organometallic Derivates of C1-Bridged Cp/Amido Titanium and Zirconium 'CpCN-Constrained Geometry' Systems" *Organometallics* **2005**, 24, 4760–4773.
- [35] J. A. Nicasio, S. Steinberg, B. Inés, M. Alcarazo, "Tuning the Lewis Acidity of Boranes in Frustrated Lewis Pair Chemistry: Implications for the Hydrogenation of Electron-Poor Alkenes" *Chemistry – A European Journal* **2013**, 19, 11016–11020.
- [36] J. E. Borger, A. W. Ehlers, M. Lutz, J. C. Slootweg, K. Lammertsma, "Stabilization and Transfer of the Transient [Mes*P4]– Butterfly Anion Using BPh₃" *Angewandte Chemie International Edition* **2016**, 55, 613–617.
- [37] R. S. Ghadwal, S. O. Reichmann, R. Herbst-Irmer, "Palladium-Catalyzed Direct C₂-Arylation of an N-Heterocyclic Carbene: An Atom-Economic Route to Mesoionic Carbene Ligands" *Chemistry – A European Journal* **2015**, 21, 4247–4251.
- [38] R. K. Harris, E. D. Becker, S. M. C. De Menezes, P. Granger, R. E. Hoffman, K. W. Zilm, "Further Conventions for NMR Shielding and Chemical Shifts (IUPAC Recommendations 2008)" *Magnetic Resonance in Chemistry* **2008**, 46, 582–598.
- [39] R. K. Harris, E. D. Becker, S. M. Cabral de Menezes, R. Goodfellow, P. Granger, "NMR nomenclature. Nuclear spin properties and conventions for chemical shifts(IUPAC Recommendations 2001)" *Pure Appl. Chem.* **2001**, 73, 1795–1818.
- [40] M. J. Frisch, G. W. Trucks, H. B. Schlegel, G. E. Scuseria, M. A. Robb, J. R. Cheeseman, G. Scalmani, V. Barone, B. Mennucci, G. A. Petersson, H. Nakatsuji, M. Caricato, X. Li, H. P. Hratchian, A. F. Izmaylov, J. Bloino, G. Zheng, J. L. Sonnenberg, M. Hada, M. Ehara, K. Toyota, R. Fukuda, J. Hasegawa, M. Ishida, T. Nakajima, Y. Honda, O. Kitao, H. Nakai, T. Vreven, J. A. Montgomery Jr, J. E. Peralta, F. Ogliaro, M. Bearpark, J. J. Heyd, E. Brothers, K. N. Kudin, V. N. Staroverov, R. Kobayashi, J. Normand, K. Raghavachari, A. Rendell, J. C. Burant, S. S. Iyengar, J. Tomasi, M. Cossi, N. Rega, J. M. Millam, M. Klene, J. E. Knox, J. B. Cross, V. Bakken, C. Adamo, J. Jaramillo, R. Gomperts, R. E. Stratmann, O. Yazyev, A. J. Austin, R. Cammi, C. Pomelli, J. W. Ochterski, R. L. Martin, K. Morokuma, V. G. Zakrzewski, G. A. Voth, P. Salvador, J. J. Dannenberg, S. Dapprich, A. D. Daniels, Ö. Farkas, J. B. Foresman, J. V. Ortiz, J. Cioslowski, D. J. Fox, "Gaussian 09, Revision E.01" *Gaussian Inc., Wallingford CT* **2009**.
- [41] F. Weigend, "Accurate Coulomb-fitting basis sets for H to Rn" *Phys. Chem. Chem. Phys.* **2006**, 8, 1057–1065.
- [42] F. Weigend, R. Ahlrichs, "Balanced basis sets of split valence, triple zeta valence and quadruple zeta valence quality for H to Rn: Design and assessment of accuracy" *Phys. Chem. Chem. Phys.* **2005**, 7, 3297–3305.
- [43] S. Grimme, "Supramolecular Binding Thermodynamics by Dispersion-Corrected Density Functional Theory" *Chemistry – A European Journal* **2012**, 18, 9955–9964.
- [44] Y.-P. Li, J. Gomes, S. Mallikarjun Sharada, A. T. Bell, M. Head-Gordon, "Improved Force-Field Parameters for QM/MM Simulations of the Energies of Adsorption for Molecules in Zeolites and a Free Rotor Correction to the Rigid Rotor Harmonic Oscillator Model for Adsorption Enthalpies" *J. Phys. Chem. C* **2015**, 119, 1840–1850.
- [45] A. V. Marenich, J. Ho, M. L. Coote, C. J. Cramer, D. G. Truhlar, "Computational electrochemistry: prediction of liquid-phase reduction potentials" *Phys. Chem. Chem. Phys.* **2014**, 16, 15068–15106.
- [46] F. Neese, "The ORCA program system" *WIREs Computational Molecular Science* **2012**, 2, 73–78.
- [47] F. Neese, "Software update: The ORCA program system—Version 5.0" *WIREs Computational Molecular Science* **2022**, 12, e1606.
- [48] A. D. Becke, "Density-functional thermochemistry. III. The role of exact exchange" *The Journal of Chemical Physics* **1993**, 98, 5648–5652.
- [49] V. Barone in *Recent Advances in Density Functional Methods*, World Scientific, **1995**, pp. 287–334.
- [50] G. M. Sheldrick, "SHELXT – Integrated space-group and crystal-structure determination" *Acta Cryst A* **2015**, 71, 3–8.
- [51] G. M. Sheldrick, "Crystal structure refinement with SHELXL" *Acta Cryst C* **2015**, 71, 3–8.
- [52] L. J. Farrugia, "ORTEP-3 for Windows - a version of ORTEP-III with a Graphical User Interface (GUI)" *J Appl Cryst* **1997**, 30, 565–565.
- [53] L. J. Farrugia, "WinGX suite for small-molecule single-crystal crystallography" *J Appl Cryst* **1999**, 32, 837–838.
- [54] P. W. Betteridge, J. R. Carruthers, R. I. Cooper, K. Prout, D. J. Watkin, "CRYSTALS version 12: software for guided crystal structure analysis" *J Appl Cryst* **2003**, 36, 1487–1487.
- [55] J. A. Ibers, W. C. Hamilton, Eds., *International Tables for X-Ray Crystallography, Vol. IV*, Kynoch Press, Birmingham, England, **1974**.

